J. Membrane Biol. 155, 11–25 (1997)

The Journal of
Membrane
Biology

© Springer-Verlag New York Inc. 1997

Cysteine Mapping in the Ion Selectivity and Toxin Binding Region of the Cardiac Na^+ Channel Pore

S.-F. Chen[1]*, H.A. Hartmann[1], G.E. Kirsch[2]

[1]Molecular Physiology and Biophysics, Baylor College of Medicine, Houston, Texas 77030

[2]Physiology and Biophysics, Rammelkamp Center for Education and Research, MetroHealth Campus, Case Western Reserve University, Cleveland, OH 44106

Received: 8 May 1996/Revised: 15 August 1996

Abstract. Aqueous exposure of critical residues in the selectivity region of voltage gated Na^+ channels was studied by cysteine-scanning mutagenesis at three positions in each of the SS2 segments of domains III (D3) and IV (D4) of the human heart Na^+ channel. Ionic currents were modified by charged cysteine-specific methanethiosulfonate (MTS) reagents, (2-aminoethyl)-methanethiosulfonate ($MTSEA^+$) and (2-sulfonatoethyl)methanethiosulfonate ($MTSES^-$) in all six of the Cys-substituted channels, including Trp → Cys substitutions at homologous positions in D3 and D4 that were predicted in secondary structure models to have buried side chains. Furthermore, in the absence of MTS modification, each of the Cys mutants showed a reduction in tetrodotoxin (TTX) block by a factor $>10^2$. Cysteine substitution without MTS modification abolished the alkali metal ion selectivity in K1418C (D3), but not in A1720C (the corresponding position in D4) suggesting that the lysine but not the alanine side chains contribute to selectivity even though both were exposed. Neither position responded to $MTSES^-$ suggesting that these residues occupy either a size- or charge-restricted region of the pore. By contrast, $MTSES^-$ markedly increased, and $MTSEA^+$ markedly decreased conductance of D1713C (D4) suggesting that the acidic side chain of Asp^{1713} acts electrostatically in an unrestricted region. These results suggest that Lys^{1418} lies in a restricted region favorable to cations, whereas Asp^{1713} is at a more peripheral location in the Na^+ channel pore.

Key words: Sodium channel — Selectivity filter — Tetrodotoxin — Saxitoxin — Surface charge — Site-directed mutagenesis — Pore

Introduction

The relationship between the guanidinium toxin receptor and the selectivity filter of Na^+ channels has been controversial. Earlier studies of low pH effects and permeability to guanidinium ions support a model (Hille, 1975), in which tetrodotoxin (TTX) and saxitoxin (STX) molecules plug their guanidinium groups into the ''selectivity filter'' that is formed in part by an acid group (Hille, 1971; Hille, 1972). However, treatment of Na^+ channels with trimethyloxonium (TMO), a carboxyl-modifying reagent, eliminated TTX and STX sensitivity, reduced single channel conductance, but left ionic selectivity and H^+-block unchanged (Spalding, 1980; Sigworth & Spalding, 1980; Worley, French & Krueger, 1986), suggesting that different carboxyls control toxin block and selectivity.

Examination of the amino acid sequence of cloned Na^+ channels led to the proposal that the regions between hydrophobic segments S5 and S6 are involved in ion selectivity and binding with guanidinium toxins, tetrodotoxin (TTX) and saxitoxin (STX) based on the presence of negatively charged residues and the predicted extracellular location (Noda et al., 1984; Guy & Seetharamulu, 1986). Mutational studies have shown that some of the residues in the short segments SS2 (Fig. 1) within the S5–S6 linkers are critical for guanidinium toxin block (Noda et al., 1989; Terlau et al., 1991; Kontis & Goldin, 1993) and ionic selectivity (Heinemann et al., 1992*b*). Furthermore, a cysteine residue in the SS2 of domain I (D1) has been shown to be the molecular de-

* *Present address:* Department of Pharmacology, University of Washington, Seattle, WA 98195

Correspondence to: G.E. Kirsch

terminant of the 10^2–10^3-fold differences in sensitivity to block by TTX, STX, and group IIB divalent cations between cardiac muscle Na^+ channels. (Brown, Lee & Powell, 1981; Frelin et al., 1986), and their brain or skeletal muscle counterparts that have an aromatic substitution at the critical position (Satin et al., 1992; Backx et al., 1992; Heinemann, Terlau & Imoto, 1992*a;* Chen et al., 1992). The results of the mutational analysis have been incorporated into a model of the Na^+ channel pore in which an antiparallel β-hairpin structure (Fig. 1) has been proposed to form the binding pocket of guanidinium toxins (Lipkind & Fozzard, 1994). In this model, D1 and D2 are symmetrically arranged with three residues in the SS2 pointing their side chains toward the tunnel; D3 and D4 are symmetrically arranged with only two residues in the SS2 directing their side chains toward the tunnel.

The goal of this study was to identify exposed side chains in the selectivity region and the guanidinium toxin binding pocket of the Na^+ channel by the substituted cysteine accessibility method (Akabas et al., 1992). We selected the cardiac Na^+ channel isoform to generalize the functional significance of conserved residues previously probed in neuronal (Terlau et al., 1991) and skeletal muscle (Pérez-García et al., 1996; Chiamvimonvat et al., 1996*a*,*b*) Na^+ channels. Since the cysteine at position 373 of human heart (hH1a) Na^+ channel can be modified by cysteine-specific methanethiosulfonate (MTS) derivatives (Kirsch, Alam & Hartmann, 1994), it was substituted by a tyrosine, the equivalent residue in the skeletal muscle isoform. The C373Y mutant was then used as the control channel. The study focuses on the SS2 segments of D3 and D4 that have been suggested to provide structural determinants of the selectivity filter of the Na^+ channel (Heinemann et al., 1992*b*). A brief report of this work has appeared in abstract form (Chen, Hartmann & Kirsch, 1995).

Materials and Methods

Construction of Cysteine Mutant cDNAs

To expedite the construction of pore region cysteine mutants, hH1a was first engineered with unique silent restriction sites flanking each region of domain III and IV (D3 and D4). The sites were placed into the cDNA, as were the cysteine mutations, via a modified megaprimer polymerase chain reaction (PCR) mutagenesis technique (Aiyar & Leis, 1993) used previously for the construction of other hH1a mutants (Hartmann et al., 1994; Kirsch et al., 1994). With these silent sites, the new restriction fragments were considerably smaller than fragments of hH1a's natural sites, thus reducing the chance of PCR-induced unwanted mismatches found in larger PCR products.

In the pore region of D3, mutational primers incorporated a *Nsi*I site into hH1a cDNA by changing the codons for Ala^{1325} and Leu^{1326} and a *Bcl*I site by changing the codon for Val^{1467}. For the pore region of D4, mutational primers placed a *Sna*BI site into hH1a cDNA by mutating the codons for Tyr^{1680} and Val^{1681} and a *Bfr*I site by mutating the codon for Leu^{1785}. After one site in each domain had been engineered and amplified, the resultant PCR product became the template for PCR of the other pore-flanking site. The mutated cassettes were ligated into hH1a cDNA at natural cloning sites also encompassed in the PCR product: *Nde*I and *Bst*EII for D3 and *Bst*EII and *Sfi*I for D4. Recombinant clones were screened by double-stranded sequence analysis of each entire ligated cassette for confirmation that only bases directed by the mutational oligonucleotides had been changed. The point mutation, C373Y of D1 (Kirsch et al., 1994), was incorporated into both of D3 and D4 silent site constructs by the ligation of the *Xho*I and *Eco*RI restriction fragment. These full-length, C373YTyr cDNAs with the new sites were transcribed and expression of their cRNA in oocytes confirmed a Cys373Y hH1a phenotype prior to the construction of each cysteine mutant.

The silent site constructs were used as templates for each of the cysteine mutations of SS2 residues of the D3 and D4 pore regions. Similar oligonucleotide-directed PCR protocols were used for the construction of each cysteine mutant. The mutated cassettes were digested with the silent restriction site enzymes and ligated into the respective silent sites of hH1a cDNA. Mutations were verified by sequence analysis of the entire ligated segment.

RNA Transcription and Oocyte Injection

5 μg of hH1a Na^+ channel cysteine mutant DNA template were linearized with *Hind*III in preparation for in vitro transcribed capped cRNA with T7 polymerase as previously reported (Hartmann et al., 1994; Drewe, Hartmann & Kirsch, 1994). Stage V or VI oocytes were defolliculated enzymatically, injected with 50 nl of cRNA solutions at an appropriate concentration. Most experiments were done on the 4th–6th day after injection. Cells with expression level, judged by the maximum peak current amplitude, in the range of 2–5 μA were used for most experiments. For experiments after cysteine-modifying reagents treatment, the expression level was adjusted upward by increasing the amount of injected cRNA to allow residual currents in the range of 2–5 μA.

Electrophysiology

Whole oocyte current was recorded by two-electrode voltage clamp using OC-725B (Warner Instrument, Hamden, CT). Beveled microelectrode tips were filled with a solution of 0.3% low melting point agarose in 3 M KCl then backfilled with 3 M KCl. Electrode resistance was in the range of 0.2 ~ 0.5 MΩ. Under these conditions step changes in membrane potential had a rise time of approximately 1 msec. The holding current at −100 mV was usually in the range of −0.06 ~ −0.25 μA. When the holding current exceeded −0.4 μA at −100 mV, the cell was discarded. The bath solution for MTS compound modification experiments consisted of (mM) NaCl 120, $MgCl_2$ 2, $CaCl_2$ 1, and HEPES 10, pH 7.2. Two MTS compounds were used in this study: the bromide salt of a positively charged compound, (2-aminoethyl)methanethiosulfonate hydrobromide ($MTSEA^+$), and the sodium salt of a negatively charged compound, sodium (2-sulfonatoethyl)methanethiosulfonate ($MTSES^-$). Both compounds were synthesized as previously described (Kirsch et al., 1994). Since the MTS compounds are unstable in aqueous solution, they were dissolved in 5 ~ 10 ml aliquot of bath solution immediately before application. The concentration was 2 mM for $MTSEA^+$ and 3 ~ 5 mM for $MTSES^-$. If the MTS compound solutions are applied several minutes after its preparation or if the perfusion rate is not fast enough, the effects of the MTS compound solutions are very different from those of freshly prepared and rapidly applied MTS compound solutions. Instead of irre-

versible effects, a reversible block on some mutants was observed, which was probably caused by hydrolyzed products of MTS compounds. To avoid these problems, the freshly prepared MTS compound solutions were applied directly into the chamber with a 1-ml dropper, immediately after the perfusion (2 ~ 3 ml/min) was switched off, and the chamber solution was exchanged with fresh MTS compound solution using the dropper 2 ~ 3 times within one min. Washout of MTS compound solution was done by switching on the bath perfusion again. This method is better than gravity perfusion that has dead space delay and short perfusion duration problems. The time course of the effects resulted from MTS compound treatment was monitored by 0.05-Hz test pulses of 16 msec stepped from −100 mV to −10 ~ −20 mV dependent on proper current amplitudes. In some cases, a series of test potentials were applied before and after MTS compound treatment so that the current-voltage relation and the reversal potential could be obtained.

For ionic selectivity experiments, test solutions of various cations were prepared by equimolar substitution of other cations for Na^+ ion in the control bath solution. The experiments were done in a paired manner. The current-voltage relation was obtained in Na^+ bath first, then the solution was switched to a different cation bath solution. After a steady state was achieved in the different cation solution, the current-voltage relation was obtained. Then the bath solution was switched back to the Na^+ bath, and the cycle was repeated again for another cation. The permeability ratio was calculated from difference between the reversal potentials obtained in the test cation solution and in control Na^+ solution obtained immediately before. TTX and STX (Calbiochem, San Diego, CA) stock solutions were diluted to various concentrations in Na^+ bath solution immediately before use. The dose-response relationship was obtained by perfusion of toxin solutions from low concentration to high concentration in a cumulative manner. The effects were monitored by 0.05-Hz test pulses until a steady-state response was obtained for each dose. Data were low-pass filtered at 5 kHz (4-pole Bessel filter, Ithaca 4302, Ithaca, NY), then digitized at 25 kHz. Linear leakage and capacitative currents were subtracted digitally using a P/4 correction method. All electrophysiological measurements were made at room temperature (22 ~ 25°C).

Data Analysis

Reversal potential (V_{rev}) was obtained by least-squares curve fitting the current-voltage relationship with the equation:

$$I = G_{max} \times (V - V_{rev}) \times (1 - (1/(1 + e^{((V-V0.5)/k)}))). \quad (1)$$

For some mutant channels, e.g., CY + K1418C, the V_{rev} is near zero and can be obtained easily. For other mutant channels, e.g., C373Y, the V_{rev} is at a very positive potential where the capacitative current is usually much larger than ionic current and it can only be estimated by extrapolation from the curve fitted with the data obtained at less positive potentials. The percent change in current amplitude after MTS compound treatment was calculated by the equation $(I_{\text{after MTSX}}/I_{\text{before MTSX}}) \times 100 - 100$. The conductance was calculated from the equation $g = I/(V - V_{rev})$, in which V_{rev} was a mean of pooled data. The percent change in conductance after MTS compound treatment was calculated by the equation $(g_{\text{after MTSX}}/g_{\text{before MTSX}}) \times 100 - 100$. The permeability ratio P_S/P_{Na} was calculated by modified Goldman-Hodgkin-Katz equation:

$$V_{rev,S} - V_{rev,Na} = 58.78 \log_{10} (P_S[S^+]/P_{Na}[Na^+]), \quad (2)$$

in which S represents a substitute monovalent cation and the temperature was 23°C. $[S^+]$ represents ionic activity that is the product of concentration and activity coefficient. The activity coefficients for Li^+, Na^+, K^+, Rb^+, Cs^+, and NH_4^+ are in the ratio of 1.02:1.00:0.99:0.98:0.97:0.97 (Hille, 1972). For dose-response measurement, the fractional current (y) *vs.* dose were fitted with the Langmuir adsorption isotherm:

$$y = 1/(1 + ([\text{toxin}]/Kd)). \quad (3)$$

The IC_{50} equals Kd in this 1:1 binding model. Data were expressed as mean ± SD unless otherwise indicated. Statistical significance of the difference between means ($P < 0.05$) was determined using ANOVA to compare each mutant channel with the control channel. Molecular dimensions were calculated using INSIGHT II software (Biosym, San Diego, CA).

Results

As shown in Fig. 1*A*, four mutations were made in the segment SS2 of domain III (D3) from the control mutant C373Y: K1418C, G1419C, W1420C, and M1421C. To simplify the wording, C373Y + K1418C is designated as K1418C and so on. The expression level of G1419C was too low (< 0.05 μA, n = 10–12 oocytes in each of three different batches) to test the effects of blockers. Four other mutations were made at the equivalent positions in the segment SS2 of domain IV (D4): A1710C, G1711C, W1712C, and D1713C. There was no detectable expression of ionic current for G1711C (n = 9–12 oocytes in each of three different batches). All the analyses were done with the remaining six mutant channels as well as the control channel. The accessibility of these substitute cysteines to extracellularly applied, positively charged MTS-ethylammonium ($MTSEA^+$) and negatively charged MTS-ethylsulfonate ($MTSES^-$) was examined first.

Effects of Cationic Modifiers on Na^+ Current

As reported previously, $MTSEA^+$ (as well as the negatively charged $MTSES^-$) slightly reduced the current amplitude of the control mutant C373Y (<15% reduction, Kirsch et al., 1994; Fig. 4*A*). This small reduction was considered to be a nonspecific effect of MTS compounds and established a control level for the interpretation of the results of other mutants. As shown in Fig. 2*A–C*, currents in all three of the SS2/D3 mutants, K1418C, W1420C, and M1421C, were markedly reduced by saturating concentrations (Kirsch et al., 1994; Pascual et al., 1995) of $MTSEA^+$ (2 mM) in a manner consistent with a covalent modification of an exposed sulfhydryl group. The residual currents after $MTSEA^+$ treatment were 17 ± 3% (n = 18), 27 ± 11% (n = 12), and 49 ± 10% (n = 16) of the pretreatment level for M1421C, W1420C, and K1418C, respectively (Fig. 4*A*). Since a steady state was not reached for K1418C (Fig. 2*C*), at least part of the residual current may come from unmodified channels. Thus, all three side chains appear to be exposed to attack by hydrophilic reagents. Furthermore, the effect at each

A

	SS1 SS2	
Domain I		
hH1a	FDSFAWAFLALFRLMTQ**D**C**W**E**R**L	355-377
rBII	FDTFSWAFLSLFRLMTQ**D**F**W**E**N**L	367-389
rSkM1	YDTFSWAFLALFRLMTQ**D**Y**W**E**N**L	383-405
Domain II		
hH1a	MMDFFHAFLIIFRILCG**E**W**I**E**T**M	881-903
rBII	MHDFFHSFLIVFRVLCG**E**W**I**E**T**M	925-947
rSkM1	MNDFFHSFLIVFRILCG**E**W**I**E**T**M	738-760
Domain III		
hH1a	FDNVGAGYLALLQVATF**K**GWMDI	1401-1423
rBII	FDNVGLGYLSLLQVATF**K**GWMDI	1405-1427
rSkM1	YDNVGLGYLSLLQVATF**K**GWMDI	1220-1242
Domain IV		
hH1a	FQTFANSMLCLFQITTS**A**GW**D**GL	1693-1415
rBII	FETFGNSMICLFQITTS**A**GW**D**GL	1697-1719
rSkM1	FETFGNSIICLFEITTS**A**GW**D**GL	1512-1534

B

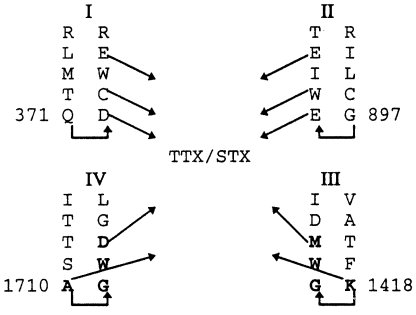

Fig. 1. The SS1–SS2 regions of Na^+ channels. (*A*) Amino acid sequence alignment of the SS1–SS2 regions (Guy & Conti, 1990) of the four domains in human heart (hH1a), rat brain (Noda et al., 1986), and rat skeletal muscle (Trimmer et al., 1989) Na^+ channel isoforms. Residues important for TTX/STX binding are bold-faced. Residues that have been suggested to be selectivity determinants are underlined. (*B*) Sequence apposition of SS1–SS2 regions in hH1a Na^+ channel according to an antiparallel β-hairpin model (Lipkind & Fozzard, 1994). Residues in SS2 segments that are predicted to expose side chains toward aqueous pore are marked by arrows. Residues that have been substituted with Cys in this study are bold-faced.

site occurred with different ON rates. For M1421C and W1420C, respectively, block reached a steady state in less than 20 sec (half effect time, $t_{1/2} < 10$ sec, $n = 18$) and in about 2 min ($t_{1/2} \approx 36 \pm 15$ sec, $n = 12$). By contrast, for K1418C block did not reach a steady state during the 7-min application ($t_{1/2} \approx 77 \pm 66$ sec, $n = 11$). Complete exchange of the bathing solution required about 15 sec, which was too slow to precisely quantify $MTSEA^+$ kinetics, but the differences in onset of the effect were very consistent and large enough to be classified as fast (for M1421C), medium (for W1420C), and slow (for K1418C).

We next tested whether residues in SS2/D4 show a pattern of exposure to $MTSEA^+$ similar to their D3 counterparts. As shown in Fig. 2*D*, $MTSEA^+$ blocks D1713C (residual current after $MTSEA^+$ treatment was 51 ± 3%, $n = 12$), in a rapid manner ($t_{1/2} < 10$ sec, $n = 12$), similar to its effect on the corresponding M1421C of D3. Also, A1710C is blocked (residual current, 77 ± 6%, $n = 7$ after treatment) with a slow onset ($t_{1/2} \approx 165 \pm 56$ sec, $n = 7$), similar to its D3 counterpart. However, W1712C (Fig. 2*E* and Fig. 4*A*), unlike its counterpart (W1420C) in D3, is not significantly different (residual current, 93 ± 29%, $n = 12$ after treatment) from control (Fig. 4*A*) in its response to $MTSEA^+$. By itself, this result suggests that the side-chain either is not exposed or that $MTSEA^+$ is excluded because of its size or charge distribution. To address this point we tested whether W1712C could be blocked by external Zn^{2+} on the basis that Zn^{2+} is a smaller probe with higher charge density than $MTSEA^+$, and because an exposed cysteine in D1 of the wild-type hH1a makes the channel highly sensitive to Zn^{2+} block ($IC_{50} \approx 30$ μM at test potential −10 mV, Kirsch et al., 1994). We found that the W1712C mutant also was sensitive to Zn^{2+} block with $IC_{50} = 310 \pm 70$ μM ($n = 7$, test potential +10 mV). The control C373Y channel, in contrast, was relatively insensitive ($IC_{50} = 3.5 \pm 1.7$ mM, $n = 5$, test potential +10 mV). These results indicate that the W1712C side chain is exposed even though it is apparently not accessible to $MTSEA^+$.

Effects of Anionic Modifiers on Na^+ Current

Block of Na^+ currents by modifiers that add a positive charge act via electrostatic repulsion as well as steric factors. By contrast, addition of a negatively charged group might be expected to either reduce current amplitude if the site of action is in a narrow region of the pore where steric hindrance is important, or enhance current amplitude if the site is in a wide region where electrostatic attraction of permeant cations is a factor. As shown in Fig. 3 both effects were observed using $MTSES^-$ depending on whether the Cys substitution was in D3 or the corresponding position in D4. Thus, both D1713C (in D4) and M1421C (in D3) could be attacked by $MTSES^-$ (Fig. 3*A* and *D*) but the effects were opposite one another: M1421C currents were blocked (residual current, 55 ± 8%, $n = 12$), whereas for D1713C, the amplitude of current increased by 27 ± 9% ($n = 17$) after $MTSES^-$ treatment (Fig. 4*B*).

The other important result obtained with $MTSES^-$ is shown in the comparison of Figs. 2*E* and 3*E*. Although the positively charged MTS compound was ineffective in W1712C (Fig. 2*E*), $MTSES^-$, substantially reduced the magnitude of the currents. In agreement with its increased sensitivity to Zn^{2+} block, the $MTSES^-$ response indicates that the residue must be exposed and readily accessible to both positive and negatively charged sulfhydryl reagents. Furthermore, as shown in Figs. 2*B* and 3*B*, the Trp of D3 is equally accessible to either $MTSEA^+$ or $MTSES^-$. Thus Cys substitutions at both of

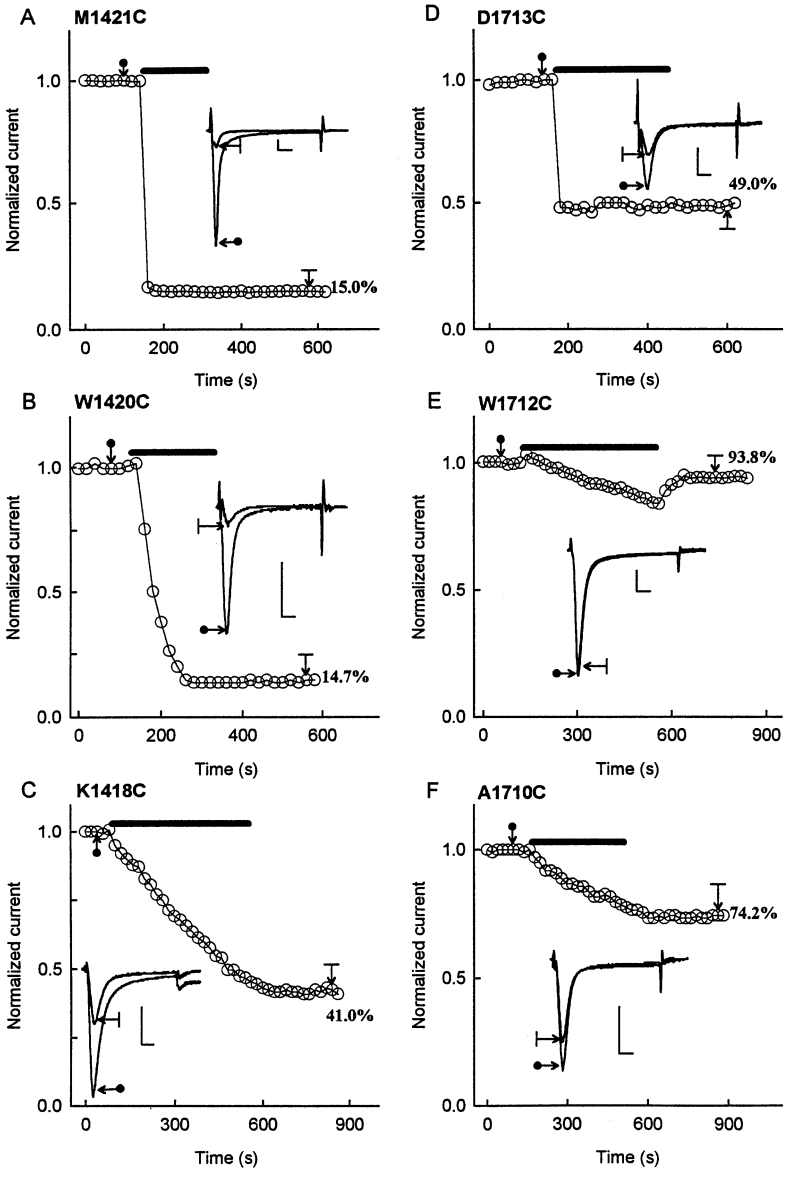

Fig. 2. Representative results of $MTSEA^+$ treatment. The current amplitudes were monitored by 0.05 Hz test pulses. The test potential is marked at the upper right corner of each panel. The current amplitudes were normalized to the pretreatment level. The percent current remained after the treatment is marked at the end of each trace. The period of $MTSEA^+$ treatment (2 mM) is marked by a horizontal bar. The scale bars for the representative current traces in each panel are 2 μA and 2 msec.

the internally homologous Trp positions appear to be accessible to MTS modification.

Finally, Fig. 3*C* and *F* shows that $MTSES^-$ had no effect on either K1418C in D3 or A1710C, the corresponding residue in D4, even though they are accessible to $MTSEA^+$. Since the volume occupied by an $MTSES^-$ molecule (93.9 Å) is about 40% larger than that of $MTSEA^+$ (67.2 Å) this result is consistent with the notion that these residues are located near the selectivity filter (Heinemann et al., 1992*b*).

Effects of Cys Substitution and MTS Reagents on Ion Selectivity

Ion selectivity in unmodified channels was evaluated by measuring the changes in reversal potential (Table 1) upon replacement of external Na^+ ions with test cations. A permeability ratio (P_S/P_{Na}, Table 2) was calculated from the modified Goldman-Hodgkin-Katz equation as described in experimental procedures. The ionic sequence for control (C373Y) is the same as that of wild type (Table 3), indicating that Cys^{373} is not involved in ion selectivity. The sequence of permeability ratio for C373Y is $Li^+ > Na^+ > K^+ > Rb^+ \approx Cs^+$ (Table 3), corresponding to Eisenman sequence XI (Hille, 1992).

We used changes in the permeability sequence as an indicator of mutation-induced changes in the selectivity. As shown in Table 3 before MTS reagent treatment, the greatest effect was observed in K1418C where the permeability sequence was altered such that the channel became nonselective amongst alkali metal cations and showed the highest permeability to ammonium, the larg-

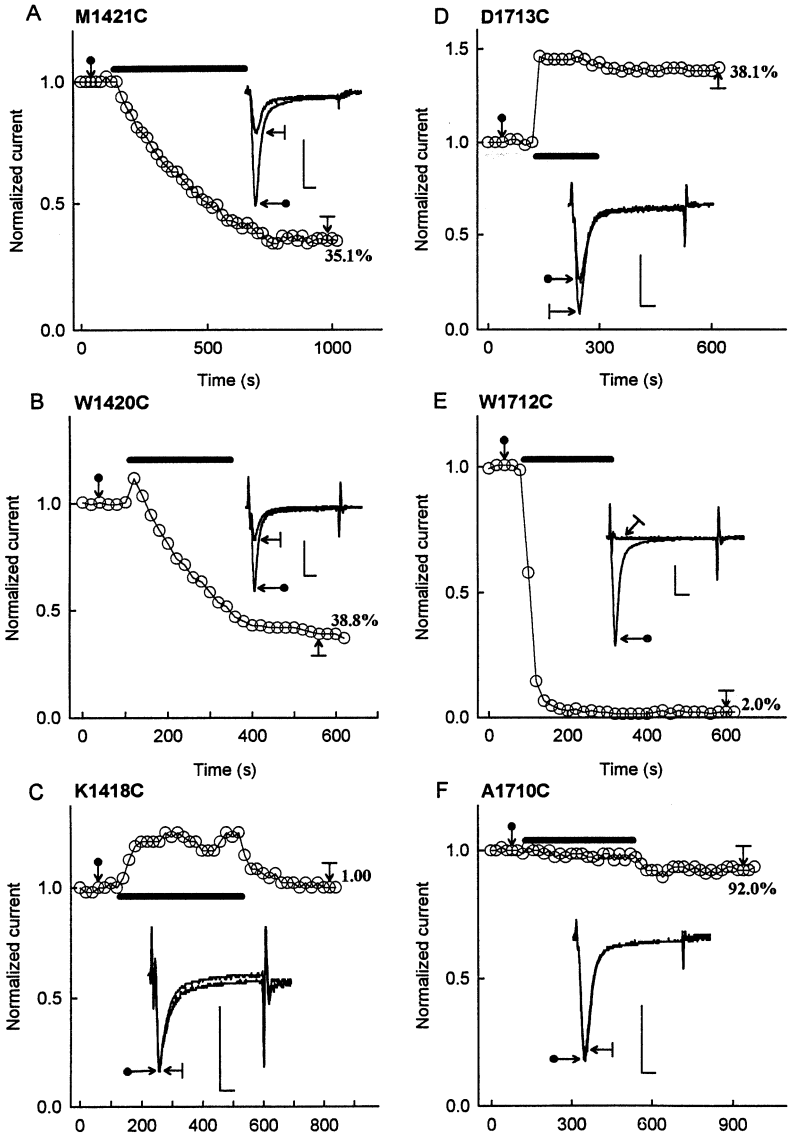

Fig. 3. Representative results of $MTSES^-$ treatment. The current amplitudes were monitored by 0.05 Hz test pulses. The test potential is marked at the upper right corner of each panel. The current amplitudes were normalized to the pretreatment level. The percent current remained or increased after the treatment is marked at the end of each trace. The period of $MTSES^-$ treatment is marked by a horizontal bar (4 mM). The scale bars for the representative current traces in each panel are 2 μA and 2 msec.

est cation tested. By contrast, the other two D3 mutations, W1420C and M1421C, retain Eisenman sequence XI. In domain IV (Table 3) before MTS treatment, all three mutants, A1710C, W1712C, and D1713C, retain Eisenman sequence XI. The results strongly support the suggestion that Lys^{1418} is located near the selectivity filter of Na^+ channels (Heinemann et al., 1992*b*) and suggest that the other five residues are not involved in ion selectivity.

The cysteine side chain after $MTSEA^+$ modification closely resembles that of lysine in terms of size and charge. We hypothesized that $MTSEA^+$ treatment of K1418C channels might reverse the mutation-induced changes in selectivity, but found that the permeability ratios were unchanged (Table 2) by either $MTSEA^+$ or $MTSES^-$. The failure of $MTSEA^+$ to restore selectivity suggests that MTS-modified channels were completely blocked and the remaining current was from unmodified channels. The lack of effects on ion selectivity after $MTSES^-$ treatment (Table 2) is consistent with the previous interpretation that this reagent could not reach K1418C.

Effects of Cysteine Substitution on TTX and STX Block

We next addressed the question of whether MTS-accessible cysteines can alter block of the channel by guanidinium toxins. Figure 5 shows the dose-response relationships of TTX and STX for the control and the six mutants. To make the comparison easier, the IC_{50} data were converted to $\Delta\Delta G$ (Fig. 5*C*). The physical meaning of $\Delta\Delta G$ is the difference in the apparent free energies of the toxin dissociation reactions between control C373Y

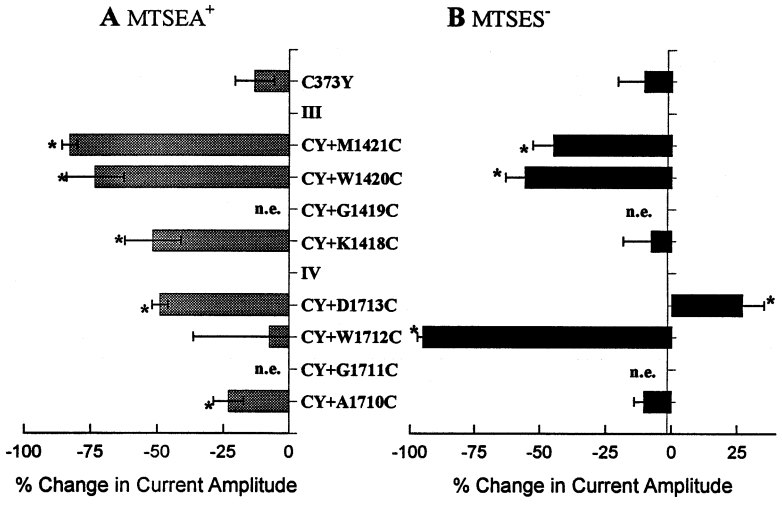

Fig. 4. Percent change in current amplitude after $MTSEA^+$ and $MTSES^-$ treatments. The percent change was calculated as described in experimental procedures. Data are presented as mean ± SD of 6–17 cells. The test potential ranges from −20 to 0 mV depending on the proper current level for each mutant. * indicates significant difference from C373Y ($P < 0.05$). n.e. indicates no expression of ionic current.

Table 1. Reversal potentials measured in Na^+ ringer solution

Mutant	Untreated	+ $MTSEA^+$ (2 mM)	+ $MTSES^-$ (3–5 mM)
C373Y	45 ± 9 ($n = 10$)		
Domain 3			
CY + K1418C	−4.9 ± 3.6 ($n = 33$)[a]	−7.1 ± 2.3 ($n = 10$)	−7.1 ± 1.3 ($n = 8$)
CY + W1420C	24 ± 6 ($n = 11$)[a]	17 ± 8 ($n = 11$)[b]	19 ± 6 ($n = 8$)
CY + M1421C	53 ± 6 ($n = 3$)	43 ± 7 ($n = 2$)	45 ± 12 ($n = 2$)
Domain 4			
CY + A1710C	55 ± 16 ($n = 3$)	34.2 ($n = 1$)	49 ± 11 ($n = 2$)
CY + W1712C	34 ± 9 ($n = 4$)	30 ± 8 ($n = 3$)	−2.3 ± 2.3 ($n = 3$)[b]
CY + D1713C	67 ± 5 ($n = 3$)[a]	68 ± 24 ($n = 2$)	53 ± 4 ($n = 3$)[b]

Data are presented as mean ± SD (mV).
[a] indicates significant difference from C373Y ($P < 0.05$).
[b] indicates significant difference from untreated cells ($P < 0.05$).

and a Cys mutant channels. A higher ΔΔG value indicates that the apparent toxin affinity of the mutant is lower than that of the control. All six mutants had lower apparent affinities to TTX than the control, with the largest reductions (three orders of magnitude) occurring in the D3 mutants, K1418C and W1420C (Fig. 5*C*). These results are consistent with the notion that the effects on TTX block extend over several residues in this region of the pore (Terlau et al., 1991). It should be noted however that the D3 residues were not equally effective in reducing TTX block; M1421C caused less than a 10-fold reduction whereas at the adjacent position W1420C caused 10^3-fold reduction. A similar pattern of reduced STX sensitivity was observed in D3 such that K1418C and W1420C showed 10^3-fold reduction in sensitivity whereas M1421C showed no change compared with control channels. These results suggest that the binding determinants for the two toxins were very similar in D3.

As shown in Fig. 5*C*, the pattern of effects was different in D4 where all three residues produced similar 10^2-fold reductions in TTX sensitivity. The pattern of responses to STX block however was markedly different from that of TTX block: A1710C and W1712C reduced STX sensitivity by 10-fold or less, whereas D1713C reduced sensitivity by at least 10^4-fold. These results support the suggestion that the negative charge of Asp^{1713} may interact with the positive charge of the 1,2,3-guanidinium group of STX (Lipkind & Fozzard, 1994). Since the C_6-OH group of TTX molecule is at a position equivalent to the 1,2,3-guanidinium group of STX (Yang & Kao, 1992) and C_6-keto derivative of TTX is less potent than TTX (Kao, 1982), the C_6-OH group of TTX molecule may interact with the carboxyl group of Asp^{1713} through hydrogen bonding. This is supported by the observation that ΔΔG of TTX for D1713C is 2.52 Kcal/mol (Fig. 5*C*), a value that is within range of hydrogen bond strength (2 ~ 10 Kcal/mol; Creighton, 1993).

We next asked whether toxin block was altered after MTS treatments at exposed residues. Based on the readily interpretable effects of charge modification at D1713C and the profound effects of this mutation on

Table 2. Permeability Ratio P_S/P_{Na}

	Li^+	K^+	NH_4^+	Rb^+	C_S^+
Untreated cells					
C373Y	1.43 ± 0.38 (4)	0.13 ± 0.03 (4)	0.29 ± 0.14 (3)	ϕ	ϕ
Domain 3					
CY + K1418C	1.22 ± 0.22 (4)	1.15 ± 0.10[a] (6)	1.64 ± 0.23[a] (6)	1.15 ± 0.11[a] (6)	0.95 ± 0.08[a] (8)
CY + W1420	1.22 ± 0.08 (4)	0.23 ± 0.05[a] (3)	0.53 ± 0.09[a] (4)	ϕ	ϕ
CY + M1421C	1.08 ± 0.10 (3)	0.058 ± 0.014[a] (3)	0.23 ± 0.09 (3)	ϕ	ϕ
Domain 4					
CY + A1710C	2.00 ± 0.28 (3)	0.044 ± 0.009[a] (2)	0.18 ± 0.03 (2)	ϕ	ϕ
CY + W1712	0.94 ± 0.13 (3)	0.17 ± 0.06 (3)	0.41 ± 0.11 (3)	ϕ	ϕ
CY + D1713C	1.03 ± 0.28 (2)	0.037 ± 0.008[a] (2)	0.11 ± 0.02 (2)	ϕ	ϕ
$MTSEA^+$-treated cells					
CY + K1418C	0.96 ± 0.01 (2)	1.19 ± 0.01 (2)	1.63 ± 0.06 (2)	1.16 ± 0.01 (2)	0.99 ± 0.01 (2)
CY + W1420	1.23 ± 0.17 (5)	0.34 ± 0.04[b] (3)	0.86 ± 0.23[b] (3)	ϕ	ϕ
CY + M1421C	0.67 ± 0.16[b] (2)	ϕ	0.28 ± 0.11 (2)	ϕ	ϕ
CY + A1710C	2.20 (2)	0.089 (1)	0.23 (1)	ϕ	ϕ
CY + W1712	0.92 ± 0.18 (2)	0.16 ± 0.01 (2)	0.34 ± 0.09 (2)	ϕ	ϕ
CY + D1713C	0.67 ± 0.41 (2)	ϕ	0.15 (1)	ϕ	ϕ
$MTSES^-$ treated cells					
CY + K1418C	0.98 (1)	1.15 ± 0.02 (2)	1.68 (1)	1.10 ± 0.04 (2)	0.99 ± 0.04 (2)
CY + W1420	1.31 ± 0.20 (3)	0.28 ± 0.08 (3)	0.73 ± 0.01[b] (2)	ϕ	ϕ
CY + M1421C	0.95 ± 0.04 (2)	0.083 ± 0.024 (2)	0.26 ± 0.12 (2)	ϕ	ϕ
CY + A1710C	1.86 (1)	ϕ	0.26 (1)	ϕ	ϕ
CY + W1712	ϕ	ϕ	ϕ	ϕ	ϕ
CY + D1713C	1.01 ± 0.01 (3)	ϕ	0.25 ± 0.09 (3)	ϕ	ϕ

Data are presented as mean ± SD (*n*).
ϕ indicates that this cation carried no or barely detectable inward current.
[a] indicates significant difference from C373Y ($P < 0.05$).
[b] indicates significant difference from untreated cells ($P < 0.05$).

Table 3. Effects of ion substitution on peak current ratios in normal and mutant channels

Controls	
WT	$Na^+ > Li^+ \gg NH_4^+ > K^+ \approx Rb^+ \approx Cs^+ \approx Ca^{2+} \approx Ba^{2+}$
C373Y	$Na^+ > Li^+ \gg NH_4^+ \approx K^+ \approx Rb^+ \approx Cs^+ \approx Ca^{2+} \approx Ba^{2+}$
Domain 3	
CY + K1418C	$NH_4^+ > K^+ \approx Rb^+ > Cs^+ \approx Ca^{2+} \approx Na^+ > Li^+ > Ba^{2+}$
CY + W1420C	$Na^+ \approx Li^+ > NH_4^+ \gg K^+$ ~0 (Rb^+, Ca^{2+}, Ba^{2+})
CY + M1421C	$Na^+ > Li^+ \gg NH_4^+ > K^+ > 0$ (Rb^+, Cs^+, Ca^{2+}, Ba^{2+})
Domain 4	
CY + A1710C	$Li^+ > Na^+ \gg NH_4^+ > K^+ > 0$ (Rb^+, Cs^+, Ca^{2+}, Ba^{2+})
CY + W1712C	$Na^+ > Li^+ \gg NH_4^+ > K^+ > 0$ (Rb^+, Cs^+, Ca^{2+}, Ba^{2+})
CY + D1713C	$Na^+ > Li^+ \gg NH_4^+ > K^+ > 0$ (Rb^+, Cs^+, Ca^{2+}, Ba^{2+})

$MTSEA^+$ or $MTSES^-$ treatments did not affect the sequence of peak current amplitude ratios in any of the mutants tested ($MTSES^-$-tested W1712C could not be tested because of the low level of residual current).

toxin block we tested the effects of $MTSES^-$ and $MTSEA^+$ treatment of D1713C on toxin block of the residual currents. We hypothesized that if toxin block required a negative charge at this site, then $MTSES^-$ modified channels would show a partial restoration, whereas $MTSEA^+$ modified channels would show a further reduction of toxin sensitivity. Unexpectedly, both modifiers further reduced toxin block of residual current (Fig. 6) and the effect of $MTSES^-$ was even greater than that of $MTSEA^+$. These results suggest that charge alone does not predict toxin block at this site but rather steric effects may be important as well in view of the fact that

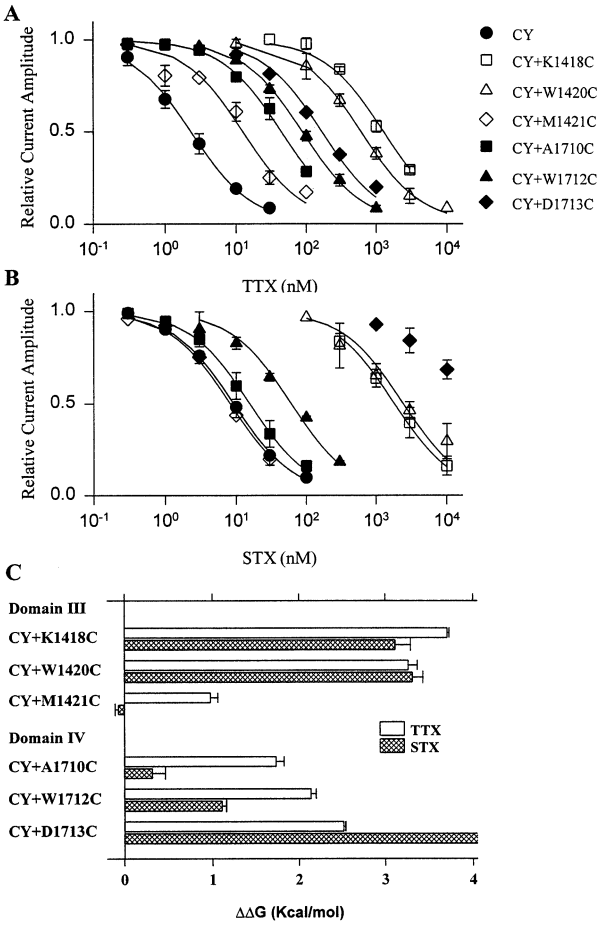

Fig. 5. Dose-response relationship and relative binding affinity of TTX and STX. (*A* and *B*) The symbols represent means obtained from 3–6 cells and the error bars represent standard deviations. The smooth curves are least-squares fit of the data with 1:1 binding model as described in experimental procedures. (*C*) The difference between the IC_{50} for each cysteine mutant and that for the control is expressed as $\Delta\Delta G$ according to the equation $\Delta\Delta G = -RT\ ln\ (IC_{50}\ for\ C373Y/IC_{50}\ for\ Cys\ mutant)$, in which $R = 1.987$ cal K^{-1} mol^{-1} and $T = 296°K$. The mean values of the IC_{50}'s for C373Y were used in these calculations. The bars represent means and the error bars represent standard deviations.

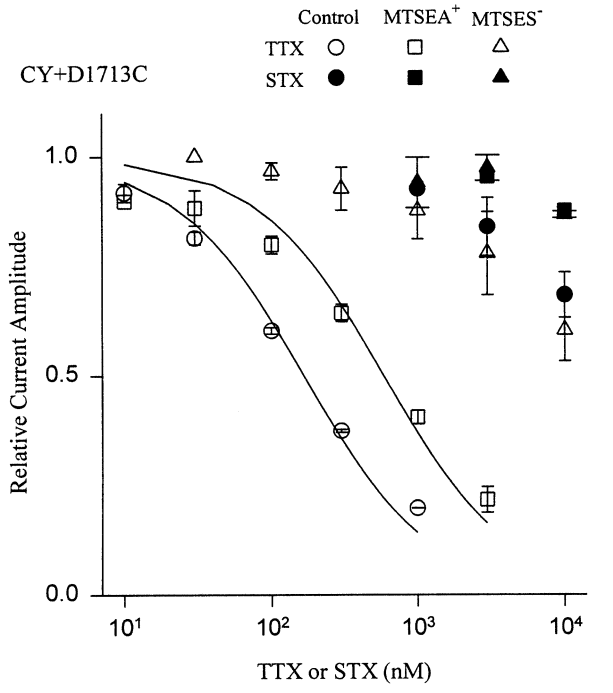

Fig. 6. The effects of $MTSEA^+$ and $MTSES^-$ on the dose-response relationships of TTX and STX for D1713C. The IC_{50} of TTX was 166 ± 6 nM (0 mV; $n = 3$), 602 ± 84 nM (0 mV; $n = 3$), and >10 μM (0 mV; $n = 4$) for untreated, $MTSEA^+$-treated, and $MTSES^-$-treated cells, respectively. The IC_{50} of STX was >10 μM for all three types of cells. The symbols represent means and the error bars represent standard deviations. The smooth curves are least squares fit of the data with 1:1 binding model.

$MTSES^-$ introduces a bulkier group (~51 $Å^3$ larger than the side chain of Met) than $MTSEA^+$ (~31 $Å^3$ larger than the side chain of Met).

Discussion

We substituted Cys residues at three corresponding loci in the SS2 pore-forming regions of domains D3 and D4. Only two of the three residues in each domain were predicted to be exposed by a model of the TTX binding site in which corresponding residues in different domains occupy equivalent positions in hairpin loops (Lipkind & Fozzard, 1994). Using MTS reagents as probes we found instead that the side chains of all six substituted cysteines were exposed. Assuming that the structure of the polypeptide backbone is maintained in the cysteine mutants, we conclude that all six residues extend their side chains toward the spatially constrained aqueous pore. Our assumption that the mutations did not cause unintended changes in higher order structure was supported by the observation that the gating in the mutant channels was unaffected. Further analysis of the mutated channels revealed qualitatively different effects of $MTSES^-$ on the homologous residues M1421C and D1713C, quantitative differences in the toxin-binding affinity between the homologous residues W1420C and W1712C, and substantial differences in ion selectivity between homologous residues K1418C and A1710C. These results are consistent with the notion that homologous residues in the SS2 of D3 and D4 are not symmetrically arranged. In addition, our results suggest that Lys^{1418} is an exposed residue of the selectivity filter, that Asp^{1713} acts electrostatically to potentiate cation conduction, and that steric factors in the SS2-lining region are critical for guanidinium toxin affinity.

Our results are readily comparable with those reported recently in studies of the skeletal muscle Na channel isoform (Pérez-García et al., 1996 and Chiamvimonvat et al., 1996*a*,*b*) in which the accessibility of substituted cysteine side-chains was probed with MTS reagents, TTX and Cd^{2+}. Pérez-García et al. (1996) also identified as being exposed all six of the residues reported here and obtained similar reductions in TTX block in mutant channels not treated with $MTSEA^+$. Particularly revealing is a comparison of the results obtained in K1418C (D3) and A1710C (D4) with their counterparts in the skeletal muscle channel. We found that the small positively charged $MTSEA^+$ reagent was an effective blocker of these mutants but the larger negatively charged $MTSES^-$ was not. Similarly in the skeletal muscle channel the analogous mutations discriminated between $MTSEA^+$ and its slightly larger analogue $MTSET^+$ such that only the smaller reagent was effective. The similarity between these findings further reinforces the notion that these residues are located in a restricted region of the pore and that this structure is conserved in all Na channels.

Our results differ from those obtained by Pérez-García et al. (1996) in two regards. A relatively minor difference is that in our experiments W1712C (D3) did not respond to $MTSEA^+$, although it was blocked by Zn^{2+} and $MTSES^-$, whereas in the skeletal muscle channel all of the Cd^{2+}-sensitive mutants including the one corresponding to W1712C also were responsive either to $MTSEA^+$ or $MTSET^+$. We have no explanation for this discrepancy other than to note that our experiments with $MTSEA^+$ for this mutant gave an unusually high amount of variability (Fig. 4*A*) and the positive response observed in the skeletal muscle channel were modest relative to most of the other positions tested. Moreover, since W1712C was sensitive to $MTSES^-$ and corresponding mutants in both channels were sensitive to Zn^{2+}, there is no disagreement about side chain exposure. A more serious discrepancy is that we saw marked changes in permeability sequence in K1418C such that all the group IA monovalent cations had equal permeability and NH_4^+ became the most permeant ion (Table 2). This result agrees with a previous report (Heinemann et al., 1992*b*) that showed drastically altered ion selectivity upon mutation of the homologous Lys in rat brain Na channels, but is at odds with Pérez-García et al. (1996) who noted that all the Cys-substituted channels including the one corresponding to K1418C are selective for Na^+ over other cations. A recent reexamination of monovalent ion selectivity in the skeletal muscle channel (Chiamvimonvat et al., 1996*b*) reported changes in peak current ratios if K1237C, similar to our results in the corresponding mutant K1418C (Table 3). Our results show that of the six residues in D3–4 only the mutation corresponding to K1418C in D3 caused a change in selectivity sequence (Table 2). By contrast, the homologous substitution of A1710C in D4 produced little change in selectivity, suggesting that it is not part of the selectivity filter, consistent with the earlier interpretation of Heinemann et al. (1992*b*) in rat brain Na channels and the recent results of Chiamvimonvat et al. (1996*b*) in rat skeletal muscle Na channels. However, Chiamvimonvat et al. (1996*b*) suggest that residues corresponding to W1712 and D1713 in D4 also may be part of the selectivity filter because of the increased I_K/I_{Na} and I_{NH4}/I_{Na} of the Cys mutants. Our results differ in that we find little or no change in permeability ratios (Table 2) for these two mutations based on whole-cell, reversal potential measurements. More complete patch-clamp measurements of reversal potentials may be necessary to determine whether these differences are methodological or real distinctions between channel isoforms.

Structural Features of the Pore Revealed by MTS Compounds

All six substituted cysteines in the SS2 of D3 and D4 could be modified by $MTSEA^+$ and/or $MTSES^-$ in this study (Table 4); but show different patterns of response. Met^{1421} and Asp^{1713} are at homologous positions in the sequence alignment; however, the effects of $MTSES^-$ treatment on M1421C and D1713C are remarkably different in two aspects. First, the modification rate for M1421C was much slower than that for either D1713C or W1712C (Fig. 3). Second, the macroscopic conductance of M1421C was decreased, but that of D1713C was increased by $MTSES^-$. A simple interpretation of the first result is that Met^{1421} is deeper and, therefore, less accessible than Asp^{1713}, resulting in a slower rate of $MTSES^-$ reaction in M1421C relative to that in D1713C. However, this kinetic difference apparently depends on the charge of the MTS reagent since the onset of $MTSEA^+$ was the same in both M1421C and D1713C (Fig. 2). We speculate that the apparent rate of the MTS reaction may be strongly influenced by the presence of nearby charged groups (e.g., Asp^{1713} in the case of M1421C) and therefore not a reliable indicator of the depth of the Cys in the pore. A stronger argument for placing the SS2 region of D4 at a shallower depth than D3 is to compare the maximum reduction in conductance resulting from saturating levels of $MTSEA^+$ (Figs. 2 and 4*A*). We found that the reduction was significantly greater for Cys substitutions in D3 than for homologous substitutions in D4. Assuming that the $MTSEA^+$ effect is due to obstruction of the pore, such a result would be expected if D3 occupied a deeper and more constricted region of the pore than D4. Chiamvimonvat et al. (1996*a*) argue that D4 is actually the deepest region on the basis of greater electrical distance estimated from the voltage dependence of Cd^{2+} block. It should be noted,

Table 4. Summary of results

	Domain III				Domain IV			
Amino acid	*K*	*G*	*W*	*M*	*A*	*G*	*W*	*D*
Residue no.	1418	1419	1420	1421	1710	1711	1712	1713
Prediction	Exposed	Buried	Buried	Exposed	Exposed	Buried	Buried	Exposed
$MTSEA^+$	−	n.d.	−	−	−	n.d.	N.E.	−
rate	slow	n.d.	interm	fast	slow	n.d.	N.E.	fast
$MTSES^-$	N.E.	n.d.	−	−	N.E.	n.d.	−	+
rate	N.E.	n.d.	slow	slow	N.E.	n.d.	interm	fast
Selectivity								
P_K/P_{Na}	++	n.d.	+	−	−	n.d.	N.E.	−
TTX block	—	n.d.	—	−	−	n.d.	−	−

Amino acid abbreviations: *K*, lysine; *G*, glycine; *W*, tryptophan; *M*, methionine; *A*, alanine; *D*, aspartate; *C*, cysteine; *Y*, tyrosine; *E*, glutamate.

Prediction, side chain aqueous accessibility according to (Lipkind & Fozzard, 1994).

$MTSEA^+$, $MTSES^-$; effect on ionic currents. *n.d.* = not determined because of barely detectable current; N.E. = No Effect; − = decrease in current amplitude; + = increase in current amplitude. rate, time course of MTS effects on ionic current.

Selectivity P_K/P_{Na}, from reversal potential, + means reduced discrimination relative to WT.

TTX block, in non-MTS treated cells, − means reduced affinity.

however, that this conclusion leads to some apparent discrepancies. For instance, A1529C (D4) was found to be accessible to $MTSEA^+$ whereas the shallower D400C (D1) was not. Conversely, the deeper position G1530C (D4), was accessible to $MTSET^+$, but the shallower positions D400C (D1) and K1237C (D3) were not. Furthermore, the fact that the apparent Cd^{2+} affinity in different Cys mutants varied 35,000-fold (1040 to 0.03 μM, Chiamvimonvat et al., 1996*a*) suggests that a single cysteinyl side chain is insufficient to form a Cd^{2+} binding site and that nearby residues also can influence the observed electrical distances.

The second of our results was that $MTSES^-$ selectively increased currents in D1713C but reduced currents in the homologous M1421C substitution in D3. The increased amplitude of current in D1713C obtained by attaching a negatively charged group, and the decreased amplitude obtained by attaching a positively charged group suggest that the Asp residue can increase the local concentration of Na^+ ions by an electrostatic effect and is suggestive of a more exterior location of this residue compared with M1421C. Our results however, do not provide evidence concerning the mechanism whereby negative surface charge contributed by Asp^{1713} affects ion conductance in the pore. We have used a simple electrostatic model to describe this effect but cannot rule out the possibility of a more complicated mechanism (Dani, 1986; Kienker et al., 1994).

The existence of fixed negative charges near the pore entrance has been suggested from the study of single channel conductance in different ionic strength conditions (Green et al., 1987). Our result provides evidence for the involvement of a specific amino acid residue. The size increase from Asp to $MTSES^-$-modified Cys (~79.0 $Å^3$) is larger than that from Met to $MTSES^-$-modified Cys (~50.9 $Å^3$), but this increase in size did not impose much physical hindrance for ionic current, consistent with the notion that Asp^{1713} is near the exterior rim of the narrow region. Neutralization of the corresponding Asp in rat brain Na^+ channels, D1717N and D1717Q, reduced single channel conductance to 57% and 43% of the wide type, respectively (Terlau et al., 1991). These results are consistent with our interpretation that steric effects on ion conduction are smaller than charge effects at this position.

To understand the implications of an exposed carboxylic acid side chain near the mouth of the channel, we have calculated the electrostatic effect of the negative charge contributed by Asp^{1701} if it were to act by a simple surface charge mechanism. The actual situation could be more complicated by factors such as the dielectric geometry of this region of the channel (Cai & Jordan, 1990). However, as a first approximation, the effects can be estimated by calculating the increase in conductance resulting from the addition of a single charge to different numbers of original charges. We assumed that the negative surface charges are located at the exterior rim of the entrance to the restricted, tunnel region. The distance between each negative surface charge and the central axis of the pore is assumed to be 6 Å, based on the model of Hille (1975). The surface potential at the center of the constriction entrance can be calculated as the sum of the Coulombic potentials generated by all the surface charges. Under these assumptions, the surface potential (ϕ_s) at the center of the exterior rim is:

$$\phi_s = -ne/4\pi\epsilon_r\epsilon_0(6\ Å),$$

in which n is the number of surface charges; ϵ_r is dielec-

tric constant of water 78.54; and ϵ_0 is vacuum permittivity. The result is $\phi_s = -n30.5$ mV. The surface concentration of Na^+ can be calculated from the Boltzmann equation:

$$C_s = C_{bulk} e^{(-ze\phi s/kT)},$$

in which $z = 1$, $C_{bulk} = 120$ mM, and T = 296°K. The results are 120 mM, 396 mM, 1.31 M, 4.33 M, and 14.3 M for $n = 0$ to 4, respectively. Under the approximation that the Na^+ channel is a singly occupied pore, the conductance-concentration relation can be described by the Michaelis-Menten equation:

$$g = g_{max}/(1 + K_{Na}C_s),$$

in which g_{max} is the saturation conductance and K_{Na} is the half-saturation concentration of Na^+ (Green & Andersen, 1991). The values of g_{max} and K_{Na} (45 pS and 1.5 M, respectively) are adopted from those estimated in canine brain Na^+ channels (Green et al., 1987). The calculated conductances (in pS) are 3.3, 9.4, 21.0, 33.4, and 40.7 for $n = 0$ to 4, respectively. The percent increase in conductance by adding one more surface charge is 182%, 123%, 59%, and 22% for $n = 0$ to 3, respectively. The 59% increase in conductance by increasing the number of surface charge from 2 to 3 is similar to the observed 55% increase in conductance obtained by $MTSES^-$ treatment of D1713C. This result is consistent with the presence of three negative surface charges near the entrance of the Na^+ channel pore. Additional charges may be supplied by Glu^{375}, Glu^{901} (Terlau et al., 1991; Chiamvimonvat et al., 1996*b*). The involvement of multiple carboxylate groups is also apparent from the observation that the carboxyl-modifying reagent TMO reduces the unitary conductance of cardiac Na^+ channels to produce three discrete levels without transitions between levels (Dudley & Baumgarten, 1993). If any one of the three acid residues is modified by TMO, the other two cannot be reached; the conductances of the channels modified at different acid residues are slightly different. As the C_s of cations can be elevated by the fixed charges, the C_s of monovalent anions will be reduced to 2.8% of C_{bulk} in the area of the external mouth. This provides an explanation for why K1418C and A1710C could not be modified by $MTSES^-$ and why W1420C and M1421C were modified by $MTSES^-$ but with slow kinetics. The area below the exterior rim of the narrow region of the pore excludes anions, possibly because of the electrostatic repulsion by the negative surface charges at Glu^{375}, Glu^{901}, and Asp^{1713} (the Met^{1421} counterparts in D1, D2, and D4, respectively).

Ion Selectivity

In Hille's model of the selectivity filter, the narrowest part of the pore is surrounded by six oxygen atoms with an area of 3.1 × 5.1 $Å^2$, in which one of the six oxygen atoms is contributed by a negatively charged carboxylate group (Hille, 1971; Hille, 1972). The latter is probably provided by Asp^{372} in the SS2 of D1, based on the observation that a neutralizing mutation, D384N, in rat brain Na^+ channels completely prevented ion conduction (Terlau et al., 1991; Pusch et al., 1991) but a similar mutation, E942Q, at the equivalent position in D2 did not affect selectivity and reduced conductance to a much lesser extent (Kontis & Goldin, 1993; Terlau et al., 1991). However, a modification of Hille's model is necessary to account for the observation that dramatic changes in ion selectivity that result from mutations K1418C (Table 3) and K1422E in a previous study (Heinemann et al., 1992*b*). We propose that a hydrogen atom from the ionized amine group of Lys^{1418} replaces one of the six oxygens in the filter. A distance of 5.1 Å is too long to allow hydrogen bond formation between the acid group and the amine group, but would permit a Na^+ ion and one water molecule to be accommodated within the selectivity filter, such that the Na^+ ion directly contacts the oxygen of the carboxylate group and the water molecule directly contacts the hydrogen of Lys^{1418}. Based on a simplified assumption that the distance between the oppositely charged centers of Na^+ and $-COO^-$ is 2 Å, the Coulombic potential energy can be estimated as −166 Kcal/mol, a value that is much larger than the −105 Kcal/mol hydration energy of Na^+ (Hille, 1992). Therefore the carboxylate group at the narrowest part of the pore may provide an energy minimum for Na^+. The positive change of Lys^{1418} may destabilize the strong attraction between Na^+ and $-COO^-$ to accelerate Na^+ flux, although the electrostatic repulsion between Na^+ and the ionized amine group is attenuated by greater distance and the dielectric properties of the intervening water molecule. In the mutant K1418C channel, the selectivity filter may be expanded from 5.1 Å to 8.5 Å, because of the shorter side chain of Cys. This enlarged filter loses its selectivity among alkali metal cations, because it can accommodate two water molecules as well as the permeant ion at the cross section, and the permeant ion is separated from the $-COO^-$ by a water molecule. The Coulombic attraction between the permeant ion and the $-COO^-$ is substantially attenuated by the larger distance and the dielectric property of the intervening water molecule; therefore, the apparent difference in size of the various cations is diminished. Ammonium is much more permeable than other alkali metal cations in K1418C because its tetrahedral structure will allow two of its four hydrogen atoms to interact with two sides of the long dimension through intervening water molecules, while the other two hydrogen atoms may interact directly with oxygen atoms at two sides of the short dimension of the selectivity filter. The oxygen atoms may be provided by

carbonyl groups at the polypeptide backbone, which can form hydrogen bonds with ammonium ions.

TTX/STX Receptor

The effects of the mutation K1418C on both ionic selectivity and guanidinium toxin binding affinities support the notion that TTX and STX plug their guanidinium groups into the selectivity filter of Na^+ channels (Hille, 1975). Our explanation for the mechanism of elimination of ionic selectivity in K1418C can also be applied to the reduction in TTX and STX block of K1418C. When the selectivity filter is enlarged, the positively charged guanidinium group can carry two water molecules at the cross section and cannot contact the acid group. Thus the electrostatic attraction between the guanidinium group and the acid group is attenuated by the greater distance between the centers of opposite charge, as well as the large dielectric constant of water molecule. The idea of multiple negative charges provides an explanation of the differential effects of TMO on ion selectivity and toxin binding affinity (Spalding, 1980). We have suggested that three exposed, carboxylates at Glu^{375}, Glu^{901}, and Asp^{1713}, can be modified by TMO, but that the two deep acid residues, Asp^{372} and Glu^{898}, cannot be reached. Previous mutational studies have shown that neutralization of any one of the four acid residues in the SS2 segments of D1 and D2 abolished the sensitivity to TTX and STX (Noda et al., 1989; Terlau et al., 1991; Kontis & Goldin, 1993), suggesting that these acidic residues are involved in direct interaction with TTX and STX. Once an exterior carboxylate is modified by TMO, the toxin binding affinities are eliminated but the ionic selectivity and H^+-block, which are determined by Asp^{372} of D1 according to our model, remain the same. The conductance decrease by TMO modification (Sigworth & Spalding, 1980; Worley III et al., 1986) may be mainly due to neutralization of one negative charge near the mouth and consequent decrease in local concentration of Na^+ ions.

The structural differences between TTX and STX have provided some useful information about the structure of Na channel pores. TTX contains only one positively charged guanidinium group while STX contains two. These two toxin molecules can be aligned by three stereospecifically similar and biologically active groups: the 1,2,3-guanidinium group, the C_9 and C_{10} hydroxyl groups of TTX; and the 7,8,9-guanidinium group and the two C_{12} hydroxyl groups of STX (Yang & Kao, 1992). When the two molecules are aligned, the 1,2,3-guanidinium group of STX is at the equivalent position as the C_6 hydroxyl group of TTX. A structure-activity study of TTX has shown that C_6 hydroxyl group is moderately active (Kao, 1982). It is still unknown if the 1,2,3-guanidinium group of STX is biologically active, but it has been proposed that 1,2,3-guanidinium group of STX interacts with the Asp^{1713} in D4 via electrostatic attraction, based on previous mutational studies (Lipkind & Fozzard, 1994). Our results support this suggestion by showing that in D1713C the $\Delta\Delta G$ of STX is not only much larger than that of TTX, but is also significantly larger than the $\Delta\Delta G$s of TTX and STX for K1418C. We propose that the C_6 hydroxyl group of TTX interacts with Asp^{1713} through hydrogen bonds, because the $\Delta\Delta G$ of TTX for D1713C is within the range of hydrogen bond energy. The interaction between a guanidinium group and a carboxyl group usually consists of not only electrostatic attractions but also hydrogen bonds (Creighton, 1993), thus, elimination of the carboxyl group in D1713C destabilizes STX more than TTX. Because Asp^{1713} is probably situated just inside the region of voltage drop in the pore (Chiamvimonvat et al., 1996*a*) and interacts most strongly with STX (Fig. 6; Terlau et al., 1991) it may be responsible for the extra voltage dependence of block by the divalent STX compared with the monovalent TTX molecules (Satin et al., 1994).

The large change in toxin block in W1420C and aqueous exposure of this side chain suggests that Trp^{1420} might interact directly with toxin. But in the absence of additional data the mechanism is unclear. Replacement of the aromatic Trp residue with Cys would eliminate the possibility of cation-π interactions (Kumpf & Dougherty, 1993; Burley & Petsko, 1996), but the large volume change and the reduced hydrophobicity resulting from this substitution might play important roles in the inhibition of toxin binding. Additional side chain substitutions would help clarify the functional role of the exposed Trp side chains in the pore.

The combination of side-chain specific modifiers and site-directed mutagenesis promises useful insights to structure-function relationships in ion channel that are not available using either technique separately. The results obtained from our combined approach suggest specific modifications of the conventional models of pore structure/function and may serve as the basis for additional tests of the molecular basis of toxin binding and ion selectivity.

We thank Wei-Qiang Dong for oocyte preparation and cRNA injection. We are also grateful to Dr. Kizhake Soman for calculating molecular dimensions. We also thank Dr. A.M. Brown for his support and encouragement. This work was supported by National Institutes of Health grant NS29473 to G.E.K. and by a grant-in-aid from the American Heart Association (Texas Affiliate) to H.A.M.

References

Aiyar, A., Leis, J. 1993. Modification of the megaprimer method of PCR mutagenesis: Improved amplification of the final product. *Biotechniques* **14:**366–369

Akabas, M.H., Stauffer, D.A., Xu, M., Karlin, A. 1992. Acetylcholine receptor channel structure probed in cysteine-substitution mutants. *Science* **258:**307–310

Backx, P.H., Yue, D.T., Lawrence, J.H., Marban, E., Tomaselli, G.F. 1992. Molecular localization of an ion-binding site within the pore of mammalian sodium channels. *Science* **257:**248–251

Brown, A.M., Lee, K.S., Powell, T. 1981. Sodium current in single rat heart muscle cells. *J. Physiol.* **318:**479–500

Burley, S.K., Petsko, G.A. 1986. Amino-aromatic interactions in proteins. *FEBS Lett.* **203:**139–143

Cai, M., Jordan, P.C. 1990. How does vestibule surface charge affect ion conduction and toxin binding in a sodium channel? *Biophys. J.* **57:**883–891

Chen, L.-Q., Chahine, M, Kallen, R.G., Barchi, R.L., Horn, R. 1992. Chimeric study of sodium channels from rat skeletal and cardiac muscle. *FEBS Lett.* **309:**253–257

Chen, S.-F., Hartmann, H.A., Kirsch, G.E. 1995. Cysteine mapping in the selectivity region of the sodium channel. *Soc. Neurosci. Abstr.* **21:**1817 (*Abstr.*)

Chiamvimonvat, N., Pérez-García, M.T., Ranjan, R., Marban, E., Tomaselli, G.F. 1996*a*. Depth asymmetries of the pore-lining segments of the Na^+ channel revealed by cysteine mutagenesis. *Neuron* **16:**1037–1047

Chiamvimonvat, N., Pérez-García, M.T., Tomaselli, G.F., Marban, E. 1996*b*. Control of ion flux and selectivity by negatively charged residues in the outer mouth of rat sodium channels. *J. Physiol.* **491:**51–59

Creighton, T.E. 1993. Proteins: Structures and molecular properties. W.H. Freeman, New York

Dani, J.A. 1986. Ion-channel entrances influence permeation. Net charge, size, shape, and binding considerations. *Biophys. J.* **49:**607–618

Drewe, J.A., Hartmann, H.A., Kirsch, G.E. 1994. Potassium channels in mammalian brain: A molecular approach. *In:* Ion channels of excitable cells. T. Narahashi, editor. pp. 243–260. Academic Press, San Diego

Dudley, S.C., Baumgarten, C.M. 1993. Modification of cardiac sodium channels by carboxyl reagents. Trimethyloxonium and water-soluble carbodiimide. *J. Gen. Physiol.* **101:**651–671

Frelin, C., Cognard, C., Vigne, P., Lazdunski, M. 1986. Tetrodotoxin-sensitive and tetrodotoxin-resistant Na^+ channels differ in their sensitivity to Cd^{2+} and Zn^{2+}. *Eur. J. Pharmacol.* **122:**245–250

Green, W.N., Andersen, O.S. 1991. Surface charges and ion channel function. *Ann. Rev. Physiol.* **53:**341–359

Green, W.N., Weiss, L.B., Andersen, O.S. 1987. Batrachotoxin-modified sodium channels in planar lipid bilayers. Ion permeation and block. *J. Gen. Physiol.* **89:**841–872

Guy, H.R., Conti, F. 1990. Pursuing the structure and function of voltage-gated channels. *Trends Neurosci.* **13:**201–206

Guy, H.R., Seetharamulu, P. 1986. Molecular model of the action potential sodium channel. *Proc. Natl. Acad. Sci. USA* **83:**508–512

Hartmann, H.A., Tiedeman, A.A., Chen, S.-F., Brown, A.M., Kirsch, G.E. 1994. Effects of III–IV linker mutations on human heart Na^+ channel inactivation gating. *Circ. Res.* **75:**114–122

Heinemann, S.H., Terlau, H., Imoto, K. 1992*a*. Molecular basis for pharmacological differences between brain and cardiac sodium channels. *Pfluegers Arch.* **422:**90–92

Heinemann, S.H., Terlau, H. Stühmer, W., Imoto, K., Numa, S. 1992*b*. Calcium channel characteristics conferred on the sodium channel by single mutations. *Nature* **356:**441–443

Hille, B. 1971. The permeability of the sodium channel to organic cations in myelinated nerve. *J. Gen. Physiol.* **58:**599–619

Hille, B. 1972. The permeability of the sodium channel to metal cations in myelinated nerve. *J. Gen. Physiol.* **59:**637–658

Hille, B. 1975. The receptor for tetrodotoxin and saxitoxin. A structural hypothesis. *Biophys. J.* **15:**615–619

Hille, B. 1992. Ionic Channels of Excitable Membranes. Sinauer Associates, Sunderland, MA

Hille, B., Woodhull, A.M., Shapiro, B.I. 1975. Negative surface charge near sodium channels of nerve: Divalent ions, monovalent ions, and pH. *Phil. Trans. R. Soc. Lond.* **270:**301–318

Kao, C.Y. 1982. Actions of nortetrodotoxin on frog muscle and squid axon. *Toxicon.* **20:**1043–1050

Kienker, P., Tomaselli, G., Jurman, M., Yellen, G. 1994. Conductance mutations of the nicotinic acetylcholine receptor do not act by a simple electrostatic mechanism. *Biophys. J.* **66:**325–334

Kirsch, G.E., Alam, M., Hartmann, H.A. 1994. Differential effects of sulfhydryl reagents on saxitoxin and tetrodotoxin block of voltage-dependent Na channels. *Biophys. J.* **67:**2305–2315

Kontis, K.J., Goldin, A.L. 1993. Site-directed mutagenesis of the putative pore region of the rat IIA sodium channel. *Mol. Pharmacol.* **43:**635–644

Kumpf, R.A., Dougherty, D.A. 1993. A mechanism for ion selectivity in potassium channels: Computational studies of cation-π interactions. *Science* **261:**1708–1710

Lipkind, G.M., Fozzard, H.A. 1994. A structural model of the tetrodotoxin and saxitoxin binding site of the Na^+ channel. *Biophys. J.* **66:**1–13

Noda, M., Ikeda, T., Kayano, T., Suzuki, H., Takeshima, H., Kurasaki, M., Takahashi, H., Numa, S. 1986. Existence of distinct sodium channel messenger RNAs in rat brain. *Nature* **320:**188–192

Noda, M., Shimizu, S., Tanabe, T., Takai, T., Kayano, T., Ikeda, T., Takahashi, H., Nakayama, H., Kanaoka, Y., Minamino, N., Kangawa, K., Matsuo, H., Raftery, M.A., Hirose, T., Inayama, S., Hayashida, H., Miyata, T., Numa, S. 1984. Primary structure of *Electrophorus electricus* sodium channel deduced from cDNA sequence. *Nature* **312:**121–127

Noda, M., Suzuki, H., Numa, S., Stühmer, W. 1989. A single point mutation confers tetrodotoxin and saxitoxin insensitivity on the sodium channel II. *FEBS Lett.* **259:**213–216

Pascual, J.M., Shieh, C.-C., Kirsch, G.E., Brown, A.M. 1995. K^+ pore structure revealed by reporter cysteines at inner and outer surfaces. *Neuron* **14:**1055–1063

Pérez-García, M.-T., Chiamvimonvat, N., Marban, E., Tomaselli, G.F. 1996. Structure of the sodium channel pore revealed by serial cysteine mutagenesis. *Proc. Natl. Acad. Sci. USA* **93:**300–304

Pusch, M., Noda, M., Stühmer, W., Numa, S., Conti, F. 1991. Single point mutations of the sodium channel drastically reduce the pore permeability without preventing its gating. *Eur. Biophys. J.* **20:**127–133

Satin, J., Kyle, J.W., Chen, M., Bell, P., Cribbs, L.L., Fozzard, H.A., Rogart, R.B. 1992. A mutant of TTX-resistant cardiac sodium channels with TTX-sensitive properties. *Science* **256:**1202–1205

Satin, J., Limgeris, J.T., Kyle, J.W., Rogart, R.B., Fozzard, H.A. 1994. The saxitoxin/tetrodotoxin binding site on cloned rat brain IIa Na channels is in the transmembrane electric field. *Biophys. J.* **67:** 1007–1014

Sigworth, F.J., Spalding, B.C. 1980. Chemical modification reduces the conductance of sodium channels in nerve. *Nature* **238:**293–295

Spalding, B.C. 1980. Properties of toxin-resistant sodium channels pro-

duced by chemical modification in frog skeletal muscle. *J. Physiol.* **305:**485–500

Terlau, H., Heinemann, S.H., Stühmer, W., Pusch, M., Conti, F., Imoto, K., Numa, S. 1991. Mapping the site of block by tetrodotoxin and saxitoxin of sodium channel II. *FEBS Lett.* **293:**93–96

Trimmer, J.S., Cooperman, S.S., Tomiko, S.A., Zhou, J., Crean, S.M., Boyle, M.B., Kallen, R.G., Sheng, Z., Barchi, R.L., Sigworth, F.J., Goodman, R.H., Agnew, W.S., Mandel, G. 1989. Primary structure and functional expression of a mammalian skeletal muscle sodium channel. *Neuron* **3:**33–49

Worley III, J.F., French, R.J., Krueger, B.K. 1986. Trimethyloxonium modification of single batrachotoxin-activated sodium channels in planar bilayers. *J. Gen. Physiol.* **87:**327–349

Yang, L., Kao, C.Y. 1992. Actions of Chiriquitoxin on frog skeletal muscle fibers and implications for the tetrodotoxin/saxitoxin receptor. *J. Gen. Physiol.* **100:**609–622